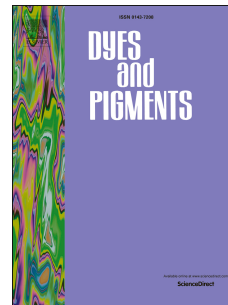


# Accepted Manuscript

Naked-eye chromogenic and fluorogenic chemosensor for mercury (II) ion based on substituted distyryl BODIPY complex

Zhaoli Xue, Tingting Liu, Huiru Liu



PII: S0143-7208(18)32399-4

DOI: <https://doi.org/10.1016/j.dyepig.2019.01.061>

Reference: DYPI 7334

To appear in: *Dyes and Pigments*

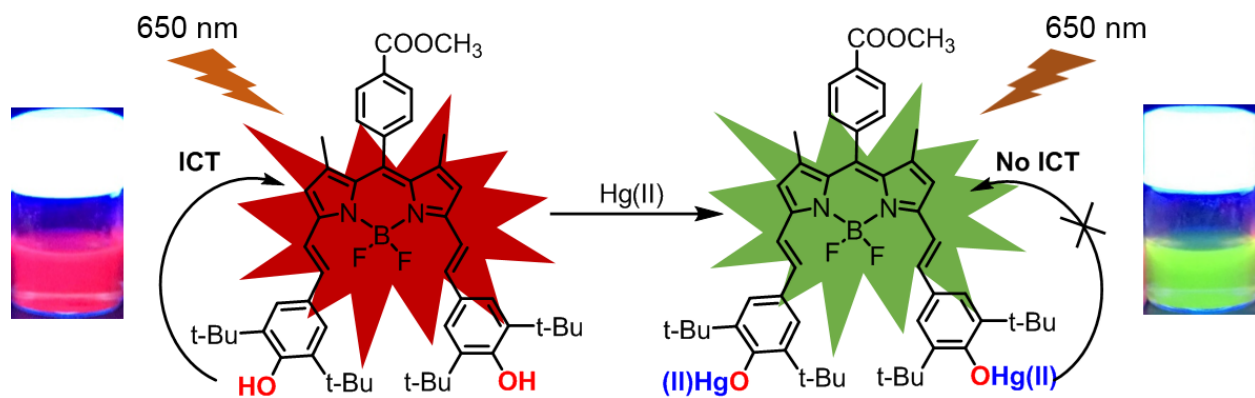
Received Date: 30 October 2018

Revised Date: 18 December 2018

Accepted Date: 31 January 2019

Please cite this article as: Xue Z, Liu T, Liu H, Naked-eye chromogenic and fluorogenic chemosensor for mercury (II) ion based on substituted distyryl BODIPY complex, *Dyes and Pigments* (2019), doi: <https://doi.org/10.1016/j.dyepig.2019.01.061>.

This is a PDF file of an unedited manuscript that has been accepted for publication. As a service to our customers we are providing this early version of the manuscript. The manuscript will undergo copyediting, typesetting, and review of the resulting proof before it is published in its final form. Please note that during the production process errors may be discovered which could affect the content, and all legal disclaimers that apply to the journal pertain.



## Naked-eye Chromogenic and Fluorogenic Chemosensor for Mercury (II) ion Based on Substituted Distyryl BODIPY Complex

Zhaoli Xue,\* Tingting Liu, Huiru Liu

*School of Chemistry and Chemical Engineering, Jiangsu University, Zhenjiang 212013, PR China*

**ABSTRACT:** One kind of novel distyryl substituted BODIPY-based fluorescent chemosensor **2** for  $\text{Hg}^{2+}$  ion sensing has been reported. Large hypsochromic shift of the absorption band is observed upon titration with  $\text{Hg}^{2+}$  ion resulting in a solution color change from green to light yellow, enabling “naked-eye” detection possible. Meanwhile, the fluorescence intensity of **2** around 680 nm was quenched upon adding  $\text{Hg}^{2+}$  ion due to the blocking of the ICT process. Most importantly, chemosensor **2** exhibits high selectivity and sensitivity towards  $\text{Hg}^{2+}$  ion over other metal ions in aqueous solutions.

**KEY WORDS:** Fluorescent sensor; Mercury(II) ion; BODIPY; Internal charge transfer (ICT); Ratiometric

### 1. Introduction

To the fact that heavy transition metal ions are high risk to the environment has been widely noted[1]. The design and synthesis of novel chemosensors for detecting heavy and toxic metal ions with artificial receptors for sensing and recognition are of great importance in environmental analyses. Recently, the development of this field has attracted considerable attention[2]. Among all the well-known heavy transition metal ions, mercury ion ( $\text{Hg}^{2+}$ ) is considered as one of the most dangerous cations for the environment due to the widespread in air, water, and soil[3]. Even more serious is that  $\text{Hg}^{2+}$  ion can be bio-accumulated through food chain and converted into organomercury, such as methylmercury ion, which will induce serious damage to the human body, especially to the central nervous system even in a low concentration[4]. Therefore, synthesis of novel chemosensors that with high selectivity and sensitivity is extremely desirable. Recently, many efforts have been made to design various chemosensors that specific for  $\text{Hg}^{2+}$  ion detection. Most of these chemosensors are based on the fact that  $\text{Hg}^{2+}$  ion is one kind of soft acid. Thus, when soft donor such as thioether[5] and dithia-dioxa-aza macrocycle[6, 7], were chosen as receptor will result in effectively selectivity to  $\text{Hg}^{2+}$  ion. But the developing of novel chemosensors that contain the receptor using hard donor such as hydroxyl group for detecting  $\text{Hg}^{2+}$  ion is still a challenge.

4,4-difluoro-4-bora-3a,4a-diaza-s-indacene (BODIPY), one of well-known porphyrin derivatives, is widely employed as a fluorescent dyes in many fields due to its advantageous in photophysical characteristics, such as intense absorption and fluorescence bands, high molar absorption coefficients, moderate fluorescence quantum yields and excellent chemostability[8-11]. Moreover, the structure of BODIPY dyes are easily to be modified which can shift the absorption and emission bands to the region that around red or near infra-red (NIR) spectral range. Recently, a particularly useful strategy of modification to the BODIPY core is introducing distyryl substituents especially with an electron-donating group (such as an amino or hydroxyl group) to form red/NIR region emitting internal charge transfer (ICT) dyes. In the case when the dyes combine with a specific metal ion, the electron-donating group loses its donating ability. Consequently, the ICT process is inhibited and the emission will be quenched and shown blue shift[12].

In this work, we are wish to report a highly selective and sensitive mercury(II) ion sensor based on

distyryl substituted BODIPYs with electron-donating dihydroxyl moieties at the 4- positions to the styryl group. The sensor behavior was investigated through both absorption and emission spectral ratiometric analyses. To the best of our knowledge, there are rare reports about the chemosensors for  $\text{Hg}^{2+}$  ion that only using hydroxyl group as donor receptor.

## 2. Experimental

### 2.1 Materials

Dichloromethane (DCM) was purchased from Aldrich Co. and used as received. All solvents and chemicals were reagent grade quality, obtained commercially and used without further purification except as noted. For spectral measurements, spectral grade dichloromethane was purchased from J&K Scientific Ltd. The solutions of metal ions were prepared from the perchlorate salts of  $\text{Na}^+$ ,  $\text{Cu}^{2+}$ ,  $\text{Ca}^{2+}$ ,  $\text{Mg}^{2+}$ ,  $\text{Zn}^{2+}$ ,  $\text{Ni}^{2+}$ ,  $\text{Pb}^{2+}$ ,  $\text{Co}^{2+}$ ,  $\text{Hg}^{2+}$ . The different salts were then dissolved in distilled water. Thin-layer chromatography (TLC), flush column chromatography, and gravity column chromatography were performed on Art. 5554 (Merck KGaA), Silica Gel 60 (Merck KGaA), and Silica Gel 60N (Kanto Chemical Co.), respectively.

### 2.2 Equipment

Melting points were measured with a Yanaco M-500D melting point apparatus.  $^1\text{H}$  and  $^{13}\text{C}$  NMR spectra were recorded in  $\text{CDCl}_3$  on a JEOL JNM-AL 400 spectrometer. Chemical shifts are reported in units of ppm relative to the solvent residue peaks ( $\text{CDCl}_3$ ,  $\delta = 7.26$  ppm for  $^1\text{H}$ , 77.16 ppm for  $^{13}\text{C}$ ). MALDI-TOF mass spectra were recorded on a Bruker Daltonics autoflexII MALDI-TOF MS spectrometer. IR and electronic absorption were recorded with Bruker Vector-22 and PerkinElmer Lambda 35 UV/Vis spectrometers, respectively.

### 2.3 Parameters for fluorescence quantum yields

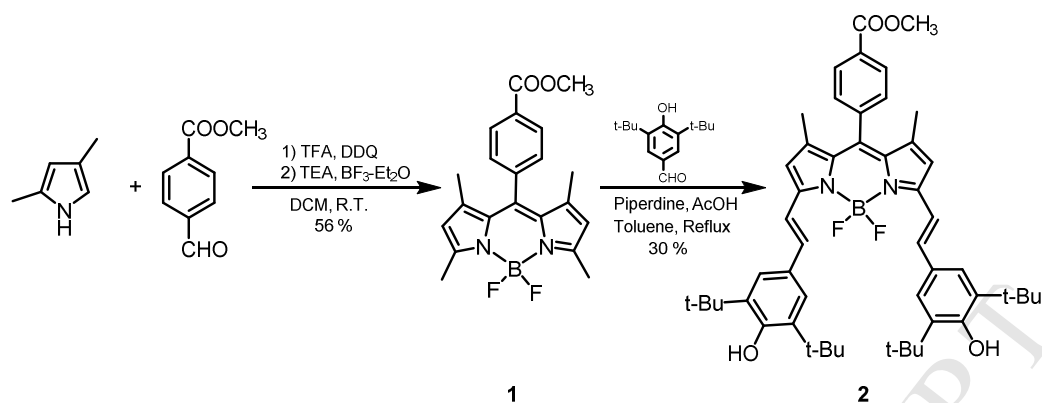
Rhodamine B was used as the standard ( $\Phi = 0.95$  in EtOH). The quantum yield,  $\Phi$ , was calculated using the following equation:

$$\Phi_{\text{sample}} = \Phi_{\text{std}} \left[ \frac{I_{\text{sample}} A_{\text{std}}}{I_{\text{std}} A_{\text{sample}}} \right] \left[ \frac{n_{\text{sample}}}{n_{\text{std}}} \right]^2$$

where the subscripts *sample* and *std* denote the sample and standard, respectively,  $\Phi$  is the quantum yield, and  $I$  is the integrated area under the corrected emission spectrum.  $A$  is the absorbance at the excitation wavelength and  $n$  is the refractive index of the solution[13].

### 2.4 Limit of detection (LOD)

The limit of detection (LOD) was calculated based on fluorescence titrations. A plot of the measured fluorescence intensity at the emission band 681 nm versus concentration of  $\text{Hg}^{2+}$  ion added allowed calculation of the limit of detection from equation  $\text{LOD} = 3\sigma/k$ , where  $\sigma$  is the standard deviation of the emission of a blank solution, which was measured three times, and  $k$  is the slope of the calibration curve[14, 15].



**Scheme 1.** Synthesis of chemosensor **2**.

### 3. Synthesis

#### 3.1 Synthesis of 1,3,5,7-tetramethyl-8-(methyl 4-benzoate)-4,4-difluoro-4-bora-3a,4a-diaza-s-indacene (**BODIPY**) **1**

Synthesis of the **1** was carried out in a one pot reaction according to the published method[16]. 2,4-dimethylpyrrole (0.75 ml, 7.57 mmol) and methyl 4-formylbenzoate (3.58 g, 21.84 mmol) were added to dry DCM (50 ml). To this mixture, 3 drops of trifluoroacetic acid (TFA) were added, and the reaction was left to stir for 4 h under Ar gas. Consumption of the methyl 4-formylbenzoate was monitored by TLC after which the temperature was lowered to 0°C, and *p*-chloranil (1.85 g, 7.57 mmol) was added. The solution was left to stir over 30 min. The temperature was lowered again to 0°C followed by the drop-wise addition of triethylamine (TEA) (2.40 ml) and BF<sub>3</sub>·Et<sub>2</sub>O (5.40 ml). After overnight stirring, the resulting solution was washed with deionized water and extracted using DCM. The dark brown solution was washed with water (3 × 20 mL) and brine (30 mL), dried over anhydrous sodium sulphate and concentrated under reduced pressure. Then the mixture was purified by silica-gel flash column chromatography (silica gel, 10 % EtOAc/Petroleum ether) and recrystallization (CHCl<sub>3</sub>/hexane) yielded red crystals of **1** (809 mg, 56 % yield). <sup>1</sup>H NMR (400 MHz, CDCl<sub>3</sub>, 298K): δ = 8.20 (d, *J* = 8.0 Hz, 2H, Ph), 7.41 (d, *J* = 8.0 Hz, 2H, Ph), 6.01 (s, 2H, pyrrole), 3.99 (s, 3H, -COOCH<sub>3</sub>), 2.58 (s, 6H, -CH<sub>3</sub>), 1.38 (s, 6H, -CH<sub>3</sub>); <sup>13</sup>C NMR (100 MHz, CDCl<sub>3</sub>, 298K) δ = 166.6, 156.1, 142.9, 140.2, 139.9, 130.9, 130.8, 130.6, 128.4, 121.8, 77.4, 77.2, 76.7, 52.8, 14.6, 14.9 ppm. MS (MALDI-TOF): Calcd for C<sub>21</sub>H<sub>21</sub>N<sub>2</sub>BF<sub>2</sub>O<sub>2</sub> [M+H]<sup>+</sup>: 383.1742, Found: 383.1745. UV-vis (in CH<sub>2</sub>Cl<sub>2</sub>) λ [nm] (ε [M<sup>-1</sup>cm<sup>-1</sup>]): 327 (10,200), 338 (10,600), 503 (42,900). Elemental Anal. Calc. for C<sub>21</sub>H<sub>21</sub>N<sub>2</sub>BF<sub>2</sub>O<sub>2</sub> requires: C, 65.99; H, 5.54; N, 7.33; Found: C, 65.82; H, 5.23; N, 7.13.

#### 3.2 4,4'-Difluoro-8-(methyl 4-benzoate)-1,7-dimethyl-2,6-diethyl-3,5-di-styryl-(3,5-di-tert-butyl-4-hydroxyphenyl)-4-bora-3a,4a-diaza-s-indacene **2**

BODIPY **1** (0.10 g, 0.26 mmole), 3,5-di-tert-butyl-4-hydroxybenzaldehyde (1.84 g, 0.78 mmol) and glacial acetic acid (0.4 mL) was added to 20 mL toluene solution under Ar. Then piperidine (0.4 mL) was added slowly, and the solution was heated to reflux for 2 h under Ar using Dean-Stark trap for the azeotropic removal of water formed during the condensation reaction. The reaction was quenched with water, then the solution was washed with water (3 × 20 mL) and brine (30 mL), dried over anhydrous sodium sulphate and concentrated at reduced pressure. Then the

mixture was purified by silica-gel flash column chromatography (silica gel, 20 % EtOAc/Petroleum ether) and recrystallization (CHCl<sub>3</sub>/hexane) yielded purple crystals of **2** (42 mg, 30 % yield). Mp: >300°C. <sup>1</sup>H NMR (400 MHz, CDCl<sub>3</sub> 298K)  $\delta$  = 8.21 (d, *J* = 8.0 Hz, 2H, Ph), 7.65 (d, *J* = 16.0 Hz, 2H, vinyl), 7.50 (d, *J* = 8.0 Hz, 2H, Ph), 8.20 (s, 4H, Ph), 7.24 (d, *J* = 16.0 Hz, 2H, vinyl), 6.64 (s, 2H, pyrrole), 5.47 (s, 2H, -OH), 4.01 (s, 3H, -COOCH<sub>3</sub>), 1.52 (s, 36H, *t*-Bu), 1.44 (s, 6H, -Me) ppm; <sup>13</sup>C NMR (100 MHz, CDCl<sub>3</sub> 298K)  $\delta$  = 166.6, 155.8, 153.4, 141.1, 140.5, 137.8, 136.9, 135.9, 130.6, 130.9, 129.1, 128.2, 124.7, 117.5, 116.8, 52.3, 34.7, 30.5, 14.7 ppm; MS (MALDI-TOF): Calcd for C<sub>51</sub>H<sub>62</sub>N<sub>2</sub>BF<sub>2</sub>O<sub>4</sub> [M+H]<sup>+</sup>: 815.4771, Found: 815.4773. UV-vis (in CH<sub>2</sub>Cl<sub>2</sub>)  $\lambda$  [nm] ( $\epsilon$  [M<sup>-1</sup>cm<sup>-1</sup>]): 322 (33,000), 377 (75,100), 603 (48,100), 653 (140,000). Elemental Anal. Calc. for C<sub>27</sub>H<sub>18</sub>N<sub>3</sub>BF<sub>2</sub> requires: C, 74.85; H, 4.19; N, 9.70; Found: C, 74.82; H, 4.13; N, 9.83.

## 4. Result and discussion

### 4.1 Synthesis and characterization

The syntheses of **1** and **2** are shown in Scheme 1. BODIPY derivative **1** was obtained following a routine formation procedure in a reasonable yield. Then the target probe, **2**, was obtained by condensation reaction of aromatic aldehyde with **1** via a one-pot Knoevenagel condensation reaction using Dean-Stark apparatus, which, after chromatographic work-up and recrystallization, was isolated in 30 % yield. The structures of **1** and **2** were characterized by NMR spectroscopy (Fig. S1-S4. in the Supp. Info.). The singlet peaks which lie at 5.47 ppm in the <sup>1</sup>H NMR spectra of **2** (Fig. S2. in the Supp. Info.), can be assigned to the -OH protons (Fig. S4. in the Supp. Info.), while the other two singlet peaks lie at 1.51 and 1.44 ppm are assigned to *t*-Bu- group and me- group, respectively.

The photophysical properties of **2** are shown in Fig.1 which were measured in THF-H<sub>2</sub>O (v:v = 1:1; HEPES 10 mM, pH= 7.2) solvent under room temperature. The most intense absorption band was found at 653 nm with the molar absorption coefficient ( $\epsilon$ )  $14.0 \times 10^4$  M<sup>-1</sup>cm<sup>-1</sup> corresponds to the low energy S<sub>0</sub>→S<sub>1</sub> transition of BODIPY core[17]. The introduction of distyryl groups to **1** caused large red-shift at about 150 nm of the typical BODIPY absorption band. Meanwhile the higher energy transitions of the molecular appeared as two weaker bands that around 322 nm and 377 nm with the molar absorption coefficient ( $\epsilon$ )  $3.3 \times 10^4$  M<sup>-1</sup>cm<sup>-1</sup> and  $7.5 \times 10^4$  M<sup>-1</sup>cm<sup>-1</sup>, respectively. The absorption spectra of complex **2** was found to be independent in common organic solvent (Fig. S5. in the Supp. Info.). The emission spectra was also measured under the same condition for absorption spectra. When excited at 650 nm, **2** exhibited emission band at 681 nm with the quantum yield of 0.89 indicates that the dye is highly fluorescent. The Stokes shift is about 28 nm which much more larger than the parent BODIPY **1** [11]. When change the solvents, the emission spectra were more affected and shown different change tendency while in *n*-C<sub>6</sub>H<sub>14</sub> cause blue-shift (664 nm) and in CH<sub>3</sub>OH shown red-shift (689 nm, Fig. S5. in the Supp. Info.).

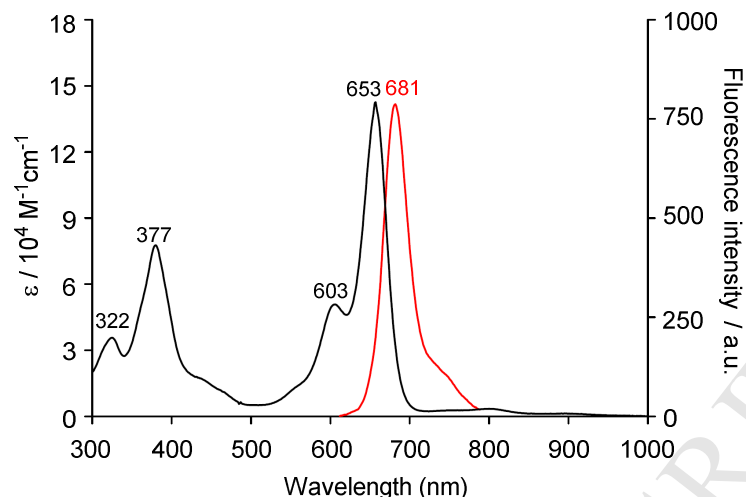


Fig. 1. Absorption and emission spectra of **2** in THF-H<sub>2</sub>O (v:v= 1:1; HEPES 10 mM, pH= 7.2) solution excited at 650 nm.

#### 4.2 Absorption spectra responses of **2** to cations

The binding properties of chemosensor **2** with different metal ions were first examined by UV-vis spectroscopy. Just as mentioned before, chemosensor **2** has two intense absorption bands at 377 nm and 653 nm in THF-H<sub>2</sub>O (v:v = 1:1; HEPES 10 mM, pH= 7.2) solution. Upon adding different kinds of metal ions to the solution that contains chemosensor **2**, no significant changes were observed. But upon addition of mercury(II) ion, red shift of the bands were observed which accompanied by the change of solution color from light green to orange (Fig. 2). This may be due to the low affinity of these ions except Hg<sup>2+</sup> ion with the receptor. Since the competitive cations did not induce any significant color changes, chemosensor **2** can be considered as an effective “naked-eye” colorimetric probe for Hg<sup>2+</sup> ion.

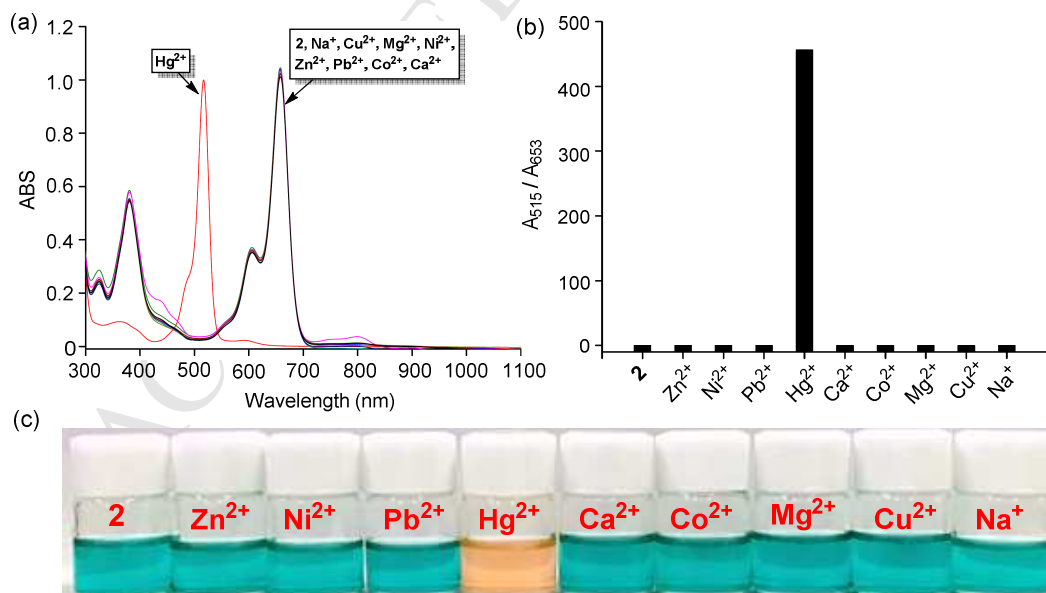
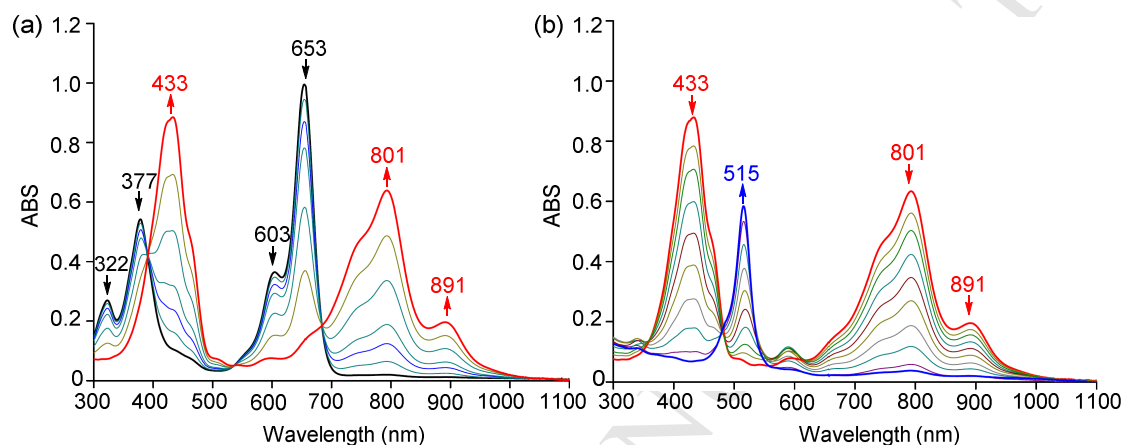


Fig. 2. (a) Normalized UV-vis spectra changes of **2** upon addition of different cations (5 equiv). (b) The absorbance ratios ( $A_{515} / A_{653}$ ) responses of chemosensor **2** containing 50 eq. of Hg<sup>2+</sup> ion to the selected different metal ions (50 eq.) (c) Color change of chemosensor **2** in the presence of different metal cations.

Moreover, titration studies were performed by adding increasing concentrations of Hg<sup>2+</sup> ion to the THF-H<sub>2</sub>O (v:v = 1:1; HEPES 10 mM, pH= 7.2) solution of chemosensor **2** (Fig. 2). Upon

titration, the coordination reaction between  $\text{Hg}^{2+}$  ion and chemosensor **2** involves a well-defined two-step process. To the first step, two intense bands at 377 nm and 653 nm decreased in intensity while two new intense bands that located at 433 nm and 801 nm intensify accompanied by another weak band near 900 nm. Interestingly, upon more  $\text{Hg}^{2+}$  ion was added, these two new intense peaks which located at 433 nm and 801 nm were replaced by the third new intense peak located at 515 nm which was similar to absorption spectra of BODIPY **1** (Fig. S6. in the Supp. Info.). The tendency of the spectra change indicated the coordination of  $\text{Hg}^{2+}$  ion to the BODIPY ligand which broke the ICT process from the distyryl groups to the BODIPY central core.



**Fig. 3.** UV-vis spectra changes of **2** upon titration by  $\text{Hg}(\text{ClO}_4)_2$  in THF- $\text{H}_2\text{O}$  ( $v:v = 1:1$ ; HEPES 10 mM, pH= 7.2). (a) first step and (b) second step.

#### 4.3 Fluorescence spectra responses of **2** to cations

In order to evaluate the fluorogenic sensing property of chemosensor **2** to  $\text{Hg}^{2+}$  ion, competition experiments and fluorescent titration studies were both carried out. As introduced before, chemosensor **2** displayed a bright red fluoresce with an intense emission band around NIR region at 681 nm (excited at 650 nm) in THF- $\text{H}_2\text{O}$  solution ( $v:v = 1:1$ ; HEPES 10 mM, pH= 7.2). When 50  $\mu\text{M}$  concentrations of various perchlorate salts of  $\text{Hg}^{2+}$ ,  $\text{Na}^+$ ,  $\text{Mg}^{2+}$ ,  $\text{Ca}^{2+}$ ,  $\text{Co}^{2+}$ ,  $\text{Ni}^{2+}$ ,  $\text{Zn}^{2+}$ ,  $\text{Pb}^{2+}$  and  $\text{Cu}^{2+}$  ions were added to the solution of chemosensor **2**, the emission intensities at 681 nm remain the same except in the presence of  $\text{Hg}^{2+}$  ion (Fig. 4). Upon adding  $\text{Hg}^{2+}$  ion the emission intensity at 681 nm was almost quenched. Such change can also be proved by exposed the solution to the UV lamp under illumination at 360 nm, the solution of **2** itself and in the presence with different metal ions shown red fluoresce. But when  $\text{Hg}^{2+}$  ion was added, the solution color changed from red to greenish which could be clearly observed by the naked-eyes (Fig. 4c). These results were consistence with UV-vis spectra change, which means chemosensor **2** shows excellent fluorescence specificity towards  $\text{Hg}^{2+}$  ion over all other different kinds of metal ions.

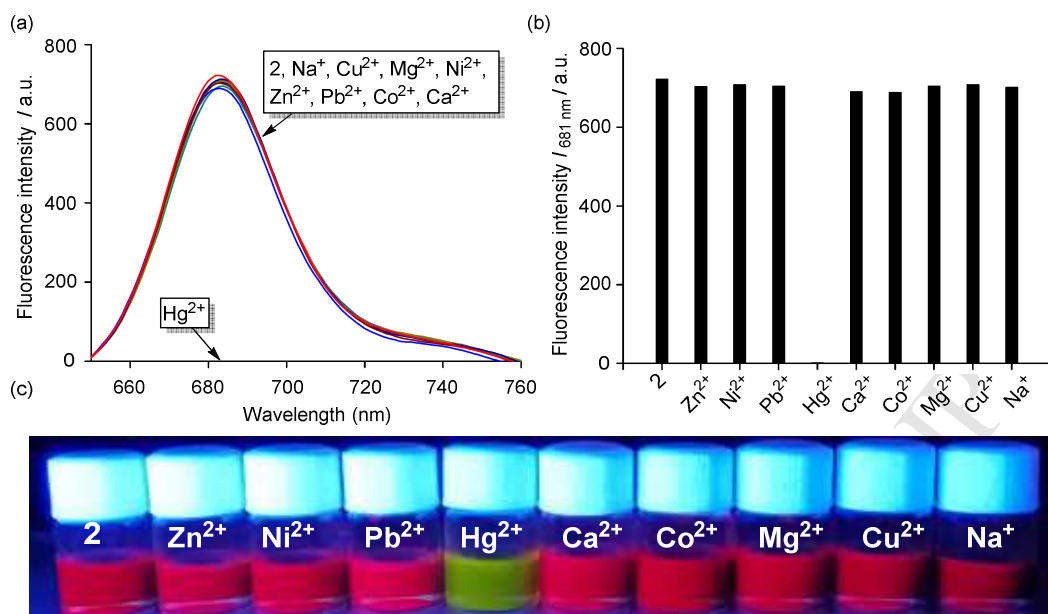


**Fig. 4.** (a) Fluorescence response of **2** in the presence of  $\text{Hg}^{2+}$  ion and other metal ion (50 eq.) in THF- $\text{H}_2\text{O}$  ( $v:v= 1:1$ ; HEPES 10 mM,  $\text{pH}= 7.2$ ) solution. The excitation wavelength was 650 nm; (b) The fluorescence responses at 681 nm ( $I_{681}$ ) of sensor **2** containing 50 eq. of  $\text{Hg}^{2+}$  ion to the selected different metal ions (50 eq.) in THF- $\text{H}_2\text{O}$  ( $v:v= 1:1$ ; HEPES 10 mM,  $\text{pH}= 7.2$ ) solution; (c) Solution colors for **2** in the presence of different metal cations illuminated with UV lamp at 360 nm.

Furthermore, fluorescence titration of chemosensor **2** with  $\text{Hg}^{2+}$  ion was also examined by adding increasing concentration of  $\text{Hg}^{2+}$  ion to THF- $\text{H}_2\text{O}$  solution ( $v:v = 1:1$ ; HEPES 10 mM,  $\text{pH}= 7.2$ ) of chemosensor **2** (Fig. 5a). The fluorescence intensity at 681 nm of chemosensor **2** was gradually decreasing upon the increasing concentration of  $\text{Hg}^{2+}$  ion. By monitoring the intensity changes at 681 nm, a typical titration curve is obtained which can be served as the calibration curve for the detection of  $\text{Hg}^{2+}$  (Fig. 5b). The detection limit was also estimated as  $0.7 \mu\text{M}$  for chemosensor **2** from the titration results (Fig. S7 in the Supp. Info.) [18]. The association constant of chemosensor **2** with  $\text{Hg}^{2+}$  ion was determined to be  $4.3 \times 10^3 \text{ M}^{-1}$  by using the Benesi-Hildebrand equation (Fig. S8 in the Supp. Info.) [19-21].

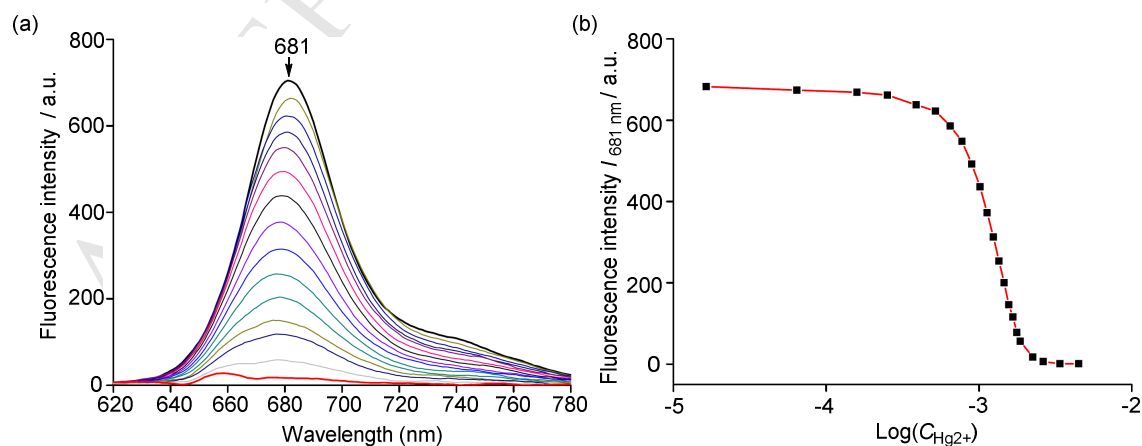


**Fig. 5.** (a) Emission spectral changes upon titration with  $\text{Hg}(\text{ClO}_4)_2$  of **2** in THF- $\text{H}_2\text{O}$  ( $v:v= 1:1$ ; HEPES 10 mM,  $\text{pH}= 7.2$ ) solution. (b) Plots of the fluorescence intensity changes at  $I_{681 \text{ nm}}$  upon different concentration of  $\text{Hg}^{2+}$  ion. Excitation wavelength was 650 nm.

#### 4.4 Investigation of the binding mode

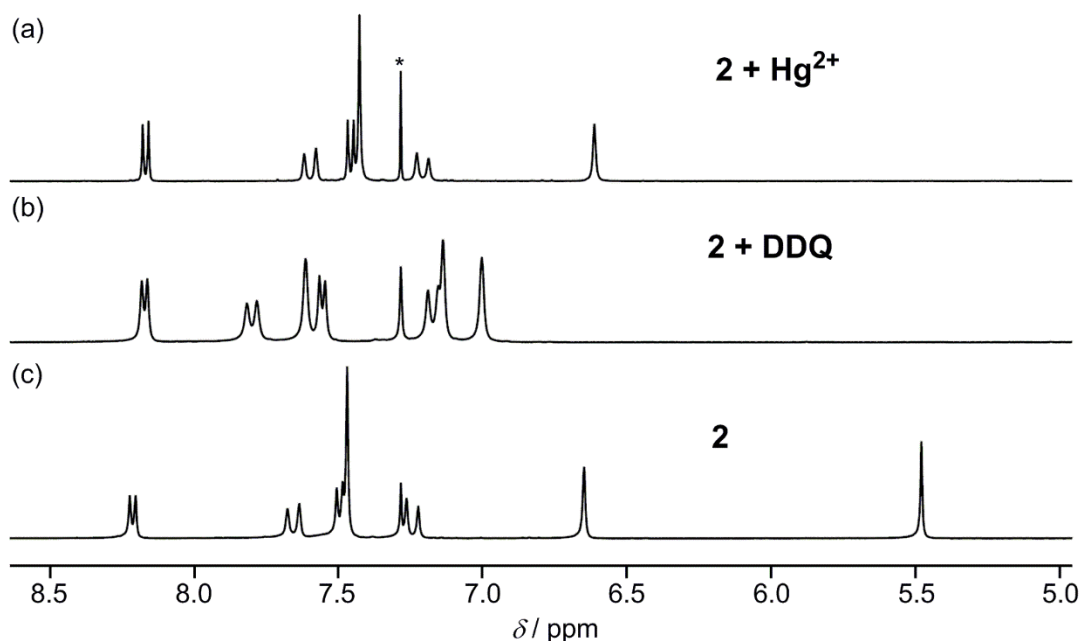


Fig. 6.  $^1\text{H}$  NMR spectra of **2** in  $\text{CDCl}_3$  at room temperature (a) **2** +  $\text{Hg}^{2+}$ , (b) **2** + **DDQ** and (c) **2** in  $\text{CDCl}_3$ . \* indicates the solvent.

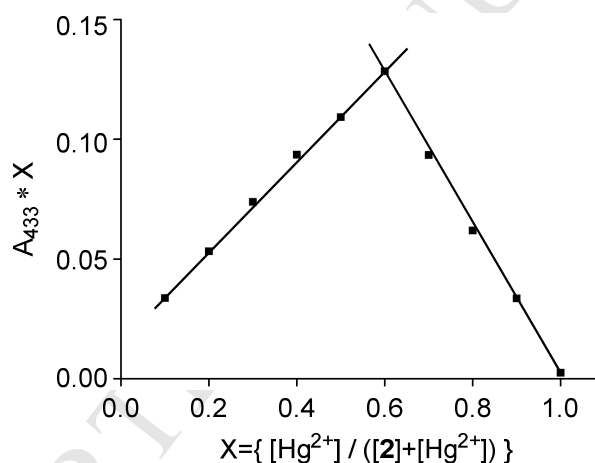


Fig. 7. Job's plot of  $\text{Hg}^{2+}$ -**2** complexes in THF- $\text{H}_2\text{O}$  (v:v= 1:1; HEPES 10 mM, pH= 7.2) solution. The monitored wavelength was 433 nm.

In order to determine the mechanism between BODIPY chemosensor **2** and  $\text{Hg}^{2+}$  ion,  $^1\text{H}$  NMR titration was employed via the addition of  $\text{Hg}^{2+}$  ion in  $\text{CDCl}_3$  at room temperature. As shown in Fig. 6a, the hydroxyl proton shown at 5.45 ppm completely disappears upon the addition of 2 equiv. of  $\text{Hg}^{2+}$  ion, while the other protons remain the same. These observations obviously indicate that the  $\text{Hg}^{2+}$  ion is coordinated to the chemosensor **2** in the ratio of 2:1. Furthermore, the formation of 2:1  $\text{Hg}^{2+}$ -**2** complex was confirmed by Job's Plot (Fig. 7). The absorption band at 433 nm was plotted against the molar fraction of chemosensor **2** under a constant total concentration. Maximum absorption intensity was reached when the molar fraction was 0.6.

But these results can't explain why during the titration process, the absorption spectra of chemosensor **2** shown two steps. Then we repeated the  $^1\text{H}$  NMR titration experiment again carefully expected to get different result. Unfortunately, we failed to get any different results. Then we try another way, we added small amount of **DDQ** (2,3-Dichloro-5,6-dicyano-1,4-benzoquinone) to the solution that contain chemosensor **2**. We

measured both the UV-vis spectra and  $^1\text{H}$  NMR spectra to the product. From the absorption spectra, we found it is just the same as compare to the first step of the titration (Fig. S9 in the Supp. Info.). The change is also proved by the  $^1\text{H}$  NMR spectra with DDQ, the phenol proton which locates at 5.4 ppm is totally disappeared while the other proton signal that locate around the region of 6.0-9.0 ppm are all shifted downfield (Fig. 6b). These information suggest that chemosensor **2** has been oxidized by DDQ to form benzoquinone structure. After we got this, we tried to purify the compound which hold the benzoquinone structure. But during the purification, we found it turned back to adopt the phenol form which indicated that the benzoquinone form is unstable. Based on these data we think the mechanism of the reaction should be: First, chemosensor **2** was oxidized by  $\text{Hg}^{2+}$  ion to form the benzoquinone structure (Fig. 6b). But the benzoquinone form is not so stable and soon went back as the phenol form which will work as didentate ligand to coordinate with  $\text{Hg}^{2+}$  ion (Fig. 6c and Fig. S10 in the Supp. Info.). After the coordination with  $\text{Hg}^{2+}$ , the ICT process from the distyryl groups to the BODIPY central core is broken. That is why the UV-spectra for final point of the titration is just like the absorption spectra of the parent complex **1**.

## 5. Conclusion

In conclusion, we have reported the synthesis and application of one kind of novel distyryl substituted BODIPY-based chromogenic and fluorescent chemosensor **2** for  $\text{Hg}^{2+}$  ion. Large hypsochromic shift of the absorption band is observed upon titration with  $\text{Hg}^{2+}$  ion resulting in a solution color change from green to light yellow, enabling “naked-eye” detection possible. Meanwhile, the fluorescence intensity of **2** around 680 nm was quenched upon adding  $\text{Hg}^{2+}$  ion due to the blocking of the ICT process. Most importantly, chemosensor **2** exhibits high selectivity and sensitivity towards  $\text{Hg}^{2+}$  ion over other metal ions in aqueous solutions. Further studies on the application of chemosensor **2** is currently underway in our laboratory.

## Author Information

E-mail: zhaolixue@ujc.edu.cn

## Acknowledgments

This work was supported by grants from the Natural Science Foundation of China (No. 21301074).

## Reference

- [1] Boening DW. Ecological effects, transport, and fate of mercury: a general review. *Chemosphere* 2000;40:1335-51.
- [2] Kim HN, Ren WX, Kim JS, Yoon J. Fluorescent and colorimetric sensors for detection of lead, cadmium, and mercury ions. *Chem Soc Rev* 2012;41:3210-44.
- [3] Di Natale F, Lancia A, Molino A, Di Natale M, Karatza D, Musmarra D. Capture of mercury ions by natural and industrial materials. *J Hazard Mater* 2006;132:220-5.
- [4] Clarkson TW, Magos L, Myers GJ. The toxicology of mercury - current exposures and clinical manifestations. *N Engl J Med* 2003;349:1731-7.
- [5] Hiruta Y, Koiso H, Ozawa H, Sato H, Hamada K, Yabushita S, Citterio D, Suzuki K. Near IR Emitting Red-Shifting Ratiometric Fluorophores Based on Borondipyrromethene. *Org Lett* 2015;17:3022-5.
- [6] Yuan M, Li Y, Li J, Li C, Liu X, Lv J, Xu J, Liu H, Wang S, Zhu D. A Colorimetric and Fluorometric Dual-Model Assay for Mercury Ion by a Molecule. *Org Lett* 2007;9:2313-6.

- [7] Coskun A, Akkaya EU. Signal Ratio Amplification via Modulation of Resonance Energy Transfer: Proof of Principle in an Emission Ratiometric Hg(II) Sensor. *J Am Chem Soc* 2006;128:14474-5.
- [8] Boens N, Leen V, Dehaen W. Fluorescent indicators based on BODIPY. *Chem Soc Rev* 2012;41:1130-72.
- [9] Kamkaew A, Lim SH, Lee HB, Kiew LV, Chung LY, Burgess K. BODIPY dyes in photodynamic therapy. *Chem Soc Rev* 2013;42:77-88.
- [10] Kowada T, Maeda H, Kikuchi K. BODIPY-based probes for the fluorescence imaging of biomolecules in living cells. *Chem Soc Rev* 2015;44:4953-72.
- [11] Lu H, Mack J, Yang Y, Shen Z. Structural modification strategies for the rational design of red/NIR region BODIPYs. *Chem Soc Rev* 2014;43:4778-823.
- [12] Coskun A, Akkaya EU. Ion Sensing Coupled to Resonance Energy Transfer: A Highly Selective and Sensitive Ratiometric Fluorescent Chemosensor for Ag(I) by a Modular Approach. *J Am Chem Soc* 2005;127:10464-5.
- [13] Olmsted J, III. Calorimetric determinations of absolute fluorescence quantum yields. *J Phys Chem* 1979;83:2581-4.
- [14] Goswami S, Das S, Aich K, Sarkar D, Mondal TK, Quah CK, Fun H-K. CHEF induced highly selective and sensitive turn-on fluorogenic and colorimetric sensor for Fe<sup>3+</sup>. *Dalton Trans* 2013;42:15113-9.
- [15] Hakonen A. Plasmon Enhancement and Surface Wave Quenching for Phase Ratiometry in Coextraction-Based Fluorosensors. *Anal Chem* 2009;81:4555-9.
- [16] Bura T, Retailleau P, Ulrich G, Ziessel R. Highly Substituted Bodipy Dyes with Spectroscopic Features Sensitive to the Environment. *J Org Chem* 2011;76:1109-17.
- [17] Yang C, Gong D, Wang X, Iqbal A, Deng M, Guo Y, Tang X, Liu W, Qin W. A new highly copper-selective fluorescence enhancement chemosensor based on BODIPY excitable with visible light and its imaging in living cells. *Sens Actuators, B* 2016;224:110-7.
- [18] Shortreed M, Kopelman R, Kuhn M, Hoyland B. Fluorescent Fiber-Optic Calcium Sensor for Physiological Measurements. *Anal Chem* 1996;68:1414-8.
- [19] Barra M, Bohne C, Scaiano JC. Effect of cyclodextrin complexation on the photochemistry of xanthone. Absolute measurement of the kinetics for triplet-state exit. *J Am Chem Soc* 1990;112:8075-9.
- [20] Benesi HA, Hildebrand JH. A spectrophotometric investigation of the interaction of iodine with aromatic hydrocarbons. *J Am Chem Soc* 1949;71:2703-7.
- [21] Zhu M, Yuan M, Liu X, Xu J, Lv J, Huang C, Liu H, Li Y, Wang S, Zhu D. Visible Near-Infrared Chemosensor for Mercury Ion. *Org Lett* 2008;10:1481-4.